C. R. Geoscience 343 (2011) 615–622

Contents lists available at ScienceDirect

Comptes Rendus Geoscience

www.sciencedirect.com

Internal geophysics

On the amplitudes of correlations and the inference of attenuations, specific intensities and site factors from ambient noise

Sur l'amplitude des corrélations et la récupération d'atténuations, d'intensités spécifiques et de facteurs de site à partir du bruit ambiant

Richard L. Weaver

Department of Physics, University of Illinois, Urbana, Illinois 61801, United States

ARTICLE INFO

Article history:
Received 1 June 2011
Accepted after revision 4 July 2011
Available online 27 August 2011

Written on invitation of the Editorial Board

Keywords:
Seismology
Attenuation
Noise correlations

ABSTRACT

While techniques for retrieval of seismic velocities from wavelet arrival times in ambient noise correlations are now well established, interpretation of wavelet amplitudes remains unsatisfactory. It is clear that such amplitudes contain information on seismic attenuation, but they are also affected by ambient noise intensity, site amplification, and any nonlinear preprocessing that may have been applied to the noise signals. Disentangling these many factors in order to reliably recover seismic attenuation is challenging. It is argued here that noise intensity, while rarely isotropic or homogeneous, may nevertheless be modeled by a radiative transfer equation. It is then shown that this recognition sufficiently constrains the noise intensity that we may hope to fit measured correlation amplitudes to models for spatially varying attenuation and site amplification factors. One-bit preprocessing, it is shown, is not compatible with such fits except in the special case of spatially constant noise intensity. An alternative procedure for accelerating convergence is suggested. Numerical simulations for a case of homogeneous attenuation and homogeneous seismic velocity are presented in support of the assertions. Attenuation, site factors, and noise intensity are successfully retrieved from correlations of numerically simulated imperfectly diffuse waves measured on a linear array of sensors.

Mots clés :
Sismologie
Atténuation
Corrélations de bruit

RÉSUMÉ

Bien que les techniques pour la récupération des vitesses sismiques dans les corrélations de bruit ambiant soient maintenant bien établies, l'interprétation des amplitudes reste insatisfaisante. Il est clair que ces amplitudes contiennent des informations sur l'atténuation sismique, mais elles sont également affectées par l'intensité du bruit ambiant, l'amplification du site et les prétraitements non linéaires. Séparer ces nombreux facteurs, pour récupérer l'atténuation sismique est un défi. Il est soutenu ici que l'intensité du bruit, bien que rarement isotrope et homogène, peut néanmoins être modélisée par une équation de transfert radiatif. Il est ensuite montré que cette reconnaissance contraint suffisamment l'intensité du bruit. En conséquence, nous pouvons récupérer l'intensité, l'atténuation et l'amplification des sites. Un prétraitement *one-bit*, comme il est montré, n'est pas compatible avec la récupération. Une autre procédure pour accélérer la convergence est suggérée. Des simulations numériques sont présentées à l'appui de ces

E-mail address: r-weaver@illinois.edu.

1631-0713/$ – see front matter
doi:10.1016/j.crte.2011.07.001

affirmations. Facteurs d'atténuation, facteurs des sites et intensité du bruit sont récupérés avec succès à partir de corrélations de simulations numériques d'ondes imparfaitement diffusées, mesurées sur un réseau linéaire de capteurs.

1. Introduction

Interest in diffuse seismic waves has seen an extraordinary growth over the last decade, driven in large part by the promise of noise correlations to reveal seismic velocities and changes in the earth's elastic properties. Key to this was the observation (Lobkis and Weaver, 2001; Weaver, 2005; Weaver and Lobkis, 2001) that fully equipartitioned diffuse waves permit, on cross-correlating the apparent noise, retrieval of the Green function, where the Green function is the signal one would have at one receiver if the other were replaced with an impulsive force. Further theoretical arguments (Roux et al., 2005a; Snieder, 2004; Wapenaar, 2004; Weaver and Lobkis, 2004), and laboratory demonstrations (Derode et al., 2003; Larose et al., 2004; Malcolm et al., 2004) in support of this conclusion quickly appeared.

Applications in long-period seismology have been particularly striking. Tomographic maps of Rayleigh wave velocity have been constructed (Lin et al., 2008; Sabra et al., 2005; Shapiro et al., 2005). The literature also reports retrieval of waveforms due to Love waves, and bulk waves (Roux et al., 2005b), and even to measures of Rayleigh wave anisotropy (Lin et al., 2008). Dense large arrays consisting of up to hundreds of seismic stations permit high resolution; the worldwide availability of their daily records for periods of years lends itself naturally to the necessary kind of data processing.

The original theoretical basis for the relation is restrictive; ambient seismic noise fields are rarely fully diffuse in the required manner. Long-period seismic noise fields are directional. Nevertheless numerous researchers report robust retrieval of travel times between distant stations, both in the lab and on the earth's surface. This is now understood as a consequence of azimuthal variations of intensity being smooth and seismic stations tending to be well separated compared to a wavelength. Quantitative details are provided by Froment et al. (2010), Godin (2009), and Weaver et al. (2009). In this asymptotic limit, travel times are largely unaffected and ambient noise directionality is unimportant. While correlations are not identical to the Green functions, the seismic velocities inferred from their direct arrivals are valid.

This robustness does not apply, however, to the amplitudes of the correlation functions. Any program to examine noise correlation amplitudes in order to infer attenuations will require a thorough understanding of the effect of noise directionality. Correlation amplitudes are also affected by site amplification factors, detector gain, and wave focusing. A program to retrieve attenuation will be challenging but the payoffs are potentially large. A successful retrieval of attenuation will necessarily also retrieve site factors and noise directionality, with implications for detecting the scattering that may have affected the directionality and determining the site factors relevant to strong ground motion (Prieto and Beroza, 2008) in earthquakes. It is towards this goal that this work is directed. For simplicity, we will confine our attention, for the present, to 2D scalar wave systems without focusing (wavespeed is homogeneous) and without scattering, and to cases in which there are linear arrays of detectors.

Prieto and Beroza (2008) and Prieto et al. (2009) suggested that azimuthal and regional averages (at fixed detector separation r) of frequency-domain normalized correlations ("coherency") can be compared to Bessel functions $J_o(\omega r/c)$ times a decaying exponential $\exp(-\alpha r)$. From this comparison, (average) wavespeed c and (average) attenuation α may be extracted. The particular genius of this approach is that it obviates concerns over noise directionality; the azimuthal average renders the ambient field effectively isotropic. It is also conjectured that such averaging mitigates the effects of focusing and defocusing. That this correlation ought look like a Bessel function J_o is well established (Aki, 1957). That deviations from a Bessel function ought be ascribable to a factor $\exp(-\alpha r)$ is less clear. Inasmuch as attenuation manifests as a complex wavespeed c, the quantity $\sqrt{r}J_o(\omega r/c)$ does not diminish with r like $\exp(-\alpha r)$. It is readily seen, e.g. by plotting it or analyzing its asymptotic form at large r, that it increases like a hyperbolic cosine or sine. It is only the causal Green function $H_o(\omega r/c)$ that decays in a manner similar to $\exp(-\alpha r)/\sqrt{r}$. There is a further concern that wavespeed c may vary with direction due to material anisotropy, or with position. An azimuthal and spatial average would correspondingly incur a spurious attenuation due to phase cancellations unrelated to anelasticity or scattering. Comparison of coherency with a theoretical form like $J_o(\omega r/c)\ \exp(-\alpha r)$ is, in this author's opinion, problematic.

Cupillard and Capdeville (2010) considered the recovery of attenuation from correlations as obtained from numerical simulations of noisy wave fields. They found, for the case of uniformly distributed noise sources (and in accord with theorems saying that such noise field correlations ought be precisely the Green function), that both geometric and intrinsic attenuation could be recovered. This was the case regardless of whether or not one-bit preprocessing was applied. They also presented numerical simulation data for the case in which the sources were distributed over a finite area patch, and for which recovering attenuation was more difficult.

As an alternative approach to retrieving amplitudes and attenuation for general noise source distributions, we here start with the theoretical form that correlation takes in a two-dimensional wave field composed of diffuse attenuating plane waves having a smoothly varying noise

directionality, or "ponderosity", $B(\theta)$ (Weaver, 2011). The amplitude of the narrow-band correlation's ray arrival from site i to site j is

$$X_{i\to j} = s_i s_j B_i(\hat{\boldsymbol{n}}_{i\to j})\sqrt{2\pi c/\omega\ |\vec{r}_i - \vec{r}_j|}\ \exp(-\ |\ \int_{\vec{r}_j}^{\vec{r}_i} \alpha dx\ |) \tag{1}$$

where the s_i are the site factors at the detectors (assumed scalar and local), and B is the intensity of the ambient wave field at site i in the direction $\hat{\boldsymbol{n}}$ towards site j. This arrival amplitude X decays geometrically and exponentially. The X differs from the amplitudes in the Green function by the presence of (not *a priori* known) prefactors B and site factors s. As indicated above and discussed by Weaver et al. (2009) and Weaver (2011), the prefactor is merely the noise intensity B in the on-strike direction. Corrections to this due to non-uniform ponderosity are negligible in the asymptotic limit that the ponderosity is smooth and the detector separations are large compared to a wavelength (Weaver, 2011). We therefore neglect such corrections here. Attenuation α in the above includes both scattering and anelasticity.

Additional influences on X may include focusing and defocusing of the ambient wavefield due to inhomogeneity of wavespeed. Here we neglect those effects and correspondingly confine the numerical examples to the case of spatially constant wave speed.

It is desired to retrieve information on α, and by implication also on B and s, from measurements of the X. This may be impossible if B is not constrained. But as discussed by Weaver (2011), B is not arbitrary; it varies in space and direction as governed by a radiative transfer equation (Ryzhik et al., 1996; Turner and Weaver, 1994) or RTE:

$$\hat{\boldsymbol{n}}\cdot\vec{\nabla}B(\vec{r},\hat{\boldsymbol{n}}) + 2\alpha(\vec{r})B(\vec{r},\hat{\boldsymbol{n}}) = \frac{1}{2\pi}\oint p\left(\hat{\boldsymbol{n}},\hat{\boldsymbol{n}}',\vec{r}\right)B\left(\vec{r},\hat{\boldsymbol{n}}'\right)d\hat{\boldsymbol{n}}' + P(\vec{r},\hat{\boldsymbol{n}}) \tag{2}$$

Ponderosity B is thus interpretable as 'specific intensity'. It is the density (per direction angle) of diffuse wave intensity. It depends on direction $\hat{\boldsymbol{n}}$ and position $\vec{r}$. Here, α is the same attenuation as in Eq. (1). The left side indicates that intensity B in a given direction decays with distance along that direction like $\exp(-2\alpha$ distance). It is noteworthy that α is responsible not only for the decay of the Green function and the noise correlation (Eq. (1)), but also for decay of the diffuse intensity B, and thus the prefactor in Eq. (1). The right side of Eq. (2) indicates that B is augmented by sources P. $B(\vec{r},\hat{\boldsymbol{n}})$ is also augmented by scattering, with strength p, into direction $\hat{\boldsymbol{n}}$ from waves at $\vec{r}$ going in direction $\hat{\boldsymbol{n}}'$. For long-period seismology P is probably zero within the continents. Whether scattering p is negligible is less clear.

Equations (1) and (2) constitute a starting point for understanding ray arrival amplitudes, and thus for retrieval of attenuation and site factors from correlations of ambient noise. Even within the approximation that focusing and defocusing are unimportant and that site factors are scalar and local, inversion from the X to the α will be non-trivial. Before attempting more general cases, however, we wish to confirm that this picture is valid by examining the particular case in which there is a linear array of sensors, arrayed along a line of direction $\pm\hat{\boldsymbol{n}}$. This is a great simplification, but it is not impractical; dense linear seismic arrays are not uncommon. In this case, the above RTE simplifies.

$$\frac{d}{dx}B^+(x) + 2\alpha(x)B^+(x) = S^+(x);$$
$$\frac{d}{dx}B^-(x) - 2\alpha(x)B^-(x) = -S^-(x) \tag{3}$$

where x is a coordinate along the linear array. Instead of an infinite number of directions, there are only two. There are two intensities of interest, $B^{\pm}$, one for each of the two directions $\pm\hat{\boldsymbol{n}}$. Each B varies along the linear array. Each attenuates exponentially at a rate 2α in its direction of travel, and is augmented by sources $S^{\pm}$. These sources may be intrinsic (P), or may be due to scattering (p) from other directions. It is particularly noteworthy that B does not decay geometrically.

The radiative transfer equation (2) simplifies even further in the case that $S = 0$, as would follow if both P and p vanish. The quantity p represents the scattering of Rayleigh waves into other Rayleigh waves and may or may not be important in practice, but for the present purposes we will assume it to be negligible. Under these conditions, B is determined entirely by two boundary values and the attenuation. It is not difficult to show that the theoretical expression for $\log X$ may then be written as a linear combination of the $\log s$, the $\log B$ at the end points of the array, and the attenuations, thus permitting inversion for these parameters. That the parameters are over-determined can be accommodated by least squares minimization (if error estimates are available on the measured X) or singular value decomposition. As such, the inversion is unique and straightforward.

Given a set of N stations, there are $N(N-1)/2$ amplitudes X associated with each of the two directions, $N(N-1)$ in all. (The auto correlations X_{ii} depend on noise intensity in all directions, not just the strike direction, and are not useful for inversion on a linear array). In the absence of effective sources S within the array, the X_{ij} depend on the two on-strike intensities at the end sites, the N site factors s_i and $N-1$ attenuations between neighboring sites. Inasmuch as the X are independent of a uniform rescaling of the s and an inverse scaling of the B, there are really only N-1 independent site factors. Thus there are $2N$ parameters to be fit by $N(N-1)$ data values. The system is over-determined if $N(N-1) > 2N$, i.e. if $N > 3$. As discussed above, the inversion is a linear process. In the presence of effective sources p or P, there are $2N-4$ additional parameters S to be fit, so the system is over-determined if $N(N-1) > 4N-4$, i.e. $N > 4$. That inversion is not linear. (Alternatively one could formulate the linear inversion of Eq. (1) without (3) in terms of $N-1$ attenuations and $2N-2$ individual values of B, and $N-1$ independent site factors s, and afterwards infer the S). In either case arrival amplitudes X between pairs in a sufficiently long array will suffice to specify all parameters of interest.

2. Numerical experiments

Numerical simulations in support of the proposed approach are carried out on a discrete 271×271 mesh representing a square two-dimensional domain. The wave equation is solved using central differences with time step dt:

$$\frac{\psi_{\vec{r}}^{t+dt} - 2\psi_{\vec{r}}^{t} + \psi_{\vec{r}}^{t-dt}}{dt^2} + \sigma_{\vec{r}} \frac{\psi_{\vec{r}}^{t+dt} - \psi_{\vec{r}}^{t-dt}}{2dt} + 4\psi_{\vec{r}}^{t} - \sum \psi_{\vec{r}'}^{t} = f_{\vec{r}}^{t} \tag{4}$$

where the vector index $\vec{r}$ indicates a site of the 271×271 mesh ($\vec{r}$ may be represented by an ordered pair of integers, each between 1 and 271), f is a time- and space-dependent forcing, and σ represents a spatially varying anelasticity. The sum is over the four nearest neighbor sites $\vec{r}'$ to $\vec{r}$.

In the absence of forcing ($f = 0$) and with constant anelasticity σ, the difference equations (4) admit plane wave solutions:

$$\psi_{\vec{r}}^{t} = \exp(i\omega t)\exp\left(-i\vec{k}\cdot\vec{r}\right) \tag{5}$$

with anisotropic dispersion relation:

$$-[2 - 2\cos(\omega dt)]/dt^2 + i\sigma\sin(\omega dt)/dt + 4 - 2\cos(k_x) - 2\cos(k_y) = 0 \tag{6}$$

For small k, i.e. long wavelengths and low frequencies, and negligible anelasticity, this is approximately $\omega^2 = k_x^2 + k_y^2$, corresponding to an isotropic medium with unit wavespeed.

The chief interest here will be in waves in the x-direction (such that $k_y = 0$) with frequency specified by a band pass filter in the vicinity of $\omega \sim 2\pi/10$. In the limit of small dt, the dispersion relation becomes

$$\omega^2 - i\sigma\omega = 2 - 2\cos(k_x) \tag{7}$$

At this frequency k_x is 0.6391 (wavelength $2\pi/k_x$ is 9.831 mesh spacings); group velocity $v_g = d\omega/dk$ is 0.9493. In the simulations discussed below σ is a constant in the interior of the mesh, at a value of 4/271. Thus Imω is 0.0074 and attenuation $\alpha = \mathrm{Im}\omega/v_g = 0.0078$ nepers per mesh spacing.

The domain is shown in Fig. 1 where the dark ring (of diameter 230 mesh spacings) represents the positions of the broadband Gaussian noise sources f. The sources are distributed uniformly in angle, at a fixed distance of 115 from the central point of the mesh. The thickness of the ring in the figure is a representation of the relative strengths of the sources (not the positions of the sources). The discrete dots indicate six receiver stations in a linear array. Attenuation is set high on the edges of the domain, to eliminate edge reflections. No scattering is included ($p = 0$). There are no sources within the array either ($P = 0$), so $S = 0$.

In order to compare with seismic scales, it is convenient to identify one time unit of the simulation (3.3 time steps dt) with one second. Assuming a seismic speed of ~3 km/sec, one identifies the mesh spacings as 3 km, such that the source ring has a diameter of 700 km and the station separations are 81 km. The simulation is run for 2^{25} time steps of d$t = 0.3$ s each, thus a scaled duration of four

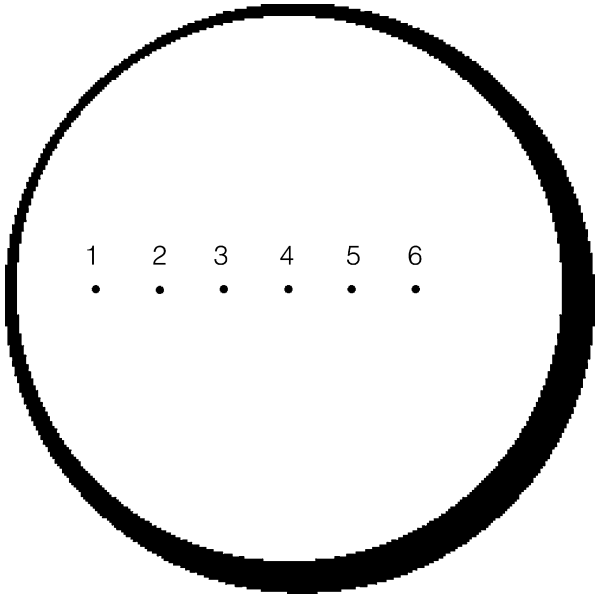

Fig. 1. Sketch of the 271×271 region on which diffuse wave field was simulated. Gaussian noise sources were distributed uniformly in angle over a ring of radius 115 and unit width. The thickness in the figure represents the source intensity $(3 + \cos(\theta + \pi/4))^2$. Thus the noise field is not isotropic. The locations of the six receiver stations (numbered 1 through 6 from left to right with interstation spacing of 27 units) are indicated by the dots.

Fig. 1. Croquis de la région sur laquelle un champ d'ondes diffuses a été simulé. Les sources de bruit Gaussien ont été distribuées sur un anneau de diamètre 230 dont l'épaisseur de la figure représente l'intensité de la source $(3 + \cos(\theta + \pi/4))^2$. Ainsi, le champ de bruit n'est pas isotrope. Les emplacements des six stations de réception (numérotés de 1 à 6 de gauche à droite, avec un espacement interstation de 27) sont indiqués par des points.

months. Fig. 2 shows a grey-scale snapshot of the wave field at a typical instant of time, with positive ψ in black and negative ψ in white. The received signal at each of the six stations was correlated with that at each of the others, filtered into a band centered on a period of 10 s (i.e. 33.3 time steps dt), stacked in the usual manner, and plotted. At this frequency, the station separation is 2.7 wavelengths. The specified attenuation corresponds to a seismic Q of 43. A typical stack is shown in Fig. 3.

3. Extraction of attenuation from the correlations

Amplitudes X are extracted from correlation waveforms like those of Fig. 3 as the root mean square (rms) of the correlation over a period from 10 s before the theoretical ray arrival time to 10 s after (20 s corresponds to the inverse bandwidth i.e. the duration of the filtered autocorrelations). While unnecessary in the present simulations as dispersion is weak, in principle the amplitude of a ray arrival ought be identified with its rms, not its peak value. Following Eq. (1), (and taking all $s = 1$) the average attenuation along the linear array can be retrieved from a fit of the log of the geometrically-corrected amplitudes *vs* distance (Fig. 4). The results agree with the known value of 0.0078 nepers/mesh spacing. The vertical offsets of different fitted lines are due to different noise intensity at different originating stations. The RTE (3)

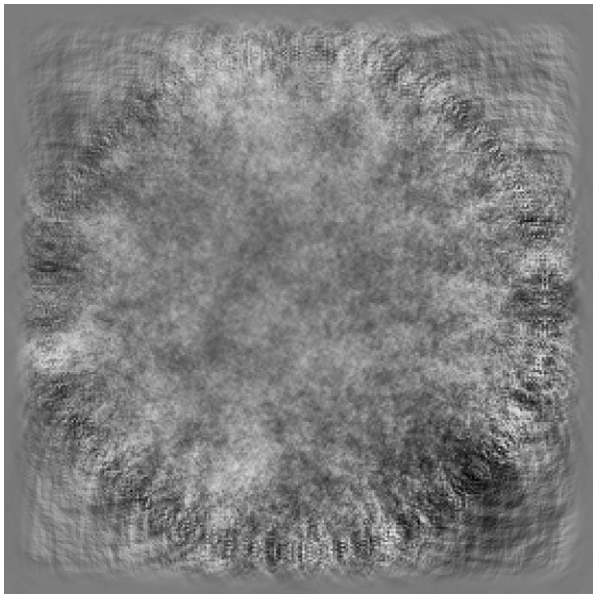

Fig. 2. Snapshot of the simulation domain at a typical instant in time. The high intensity near the sources is evident, as is the high attenuation on the edges and modest attenuation across the interior. The simulation is broadband (a band pass filter is applied to the six records before correlation processing), hence the short length scale graininess in places.

Fig. 2. Instantané du domaine de la simulation dans un instant typique. La forte intensité près des sources est évidente, comme l'est l'atténuation importante sur les bords, ou l'atténuation modeste à l'intérieur. La simulation est à large bande (un filtre bande de transition est appliqué aux six signaux avant traitement de corrélation), d'où la *graininess* de courte longueur d'onde sur l'image.

tells us that the intensity B should diminish exponentially with distance along the array like $\exp(-2\alpha * \text{distance})$, but not geometrically. This prediction is confirmed by examining the amplitudes of the adjacent pairs (Fig. 5). This simple numerical simulation demonstrates retrieval of medium attenuation and noise intensity using the approach outlined above for the case of uniform site factors s and no internal sources P or scattering p. In particular it confirms that the prefactors B are governed by a radiative transfer equation.

Similar results are obtained using the amplitudes of the correlations from left to right (for example from station 1 to other stations). One curious observation is that the amplitudes at negative lapse time in Fig. 2 are nearly constant. This is, though, consistent with theory; it is a consequence of geometric and exponential attenuation *and* the differences between the right-going noise intensities B^+ at the different stations. The rays at the negative lapse time of Fig. 3 are 5→6, ..., 1→6. The amplitudes are $B_i^+ \exp(-\alpha \text{ distance})/\text{sqrt}(\text{distance})$, where i is 5, 4, 3, 2 or 1, respectively. According to Eq. (3), B_i^+ varies like $\exp(+2\alpha \text{ distance})$. The net effect is $\exp(+\alpha \text{ distance})$ divided by the square root of distance, which is roughly constant.

4. Simultaneous inversion for attenuation, site factors, and incident intensity

The above straight line fits are illustrative, but fits to linear functions of distance like those of Figs. 4 and 5 are

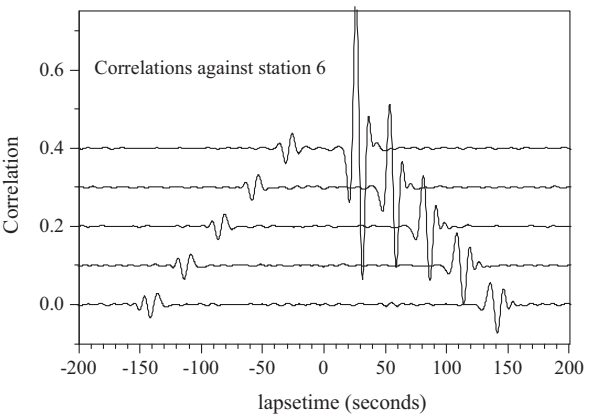

Fig. 3. Stack of correlation waveforms between station 6 (the rightmost in Fig. 1) and the five others (from top to bottom are 6–5, ..., 6–1, respectively). Temporal asymmetry is a consequence of the on-strike noise intensities in the two directions being not equal. Amplitude decay is evident at positive lapse time (propagation in direction from right to left, i.e., 6→5, ..., 6→1). It is due to both geometric attenuation and anelasticity.

Fig. 3. Addition des corrélations entre la station 6 (la plus à droite à la Fig. 1) et les cinq autres (de haut en bas, 6–5, ..., 6–1, respectivement). L'asymétrie temporelle est une conséquence des intensités du bruit, non égales dans les deux directions. La diminution de l'amplitude est évidente au temps positif (propagation dirigée de la droite vers la gauche, c'est-à-dire 6→5, ..., 6→1). Ceci est dû à la fois à l'atténuation géométrique et à l'anélasticité.

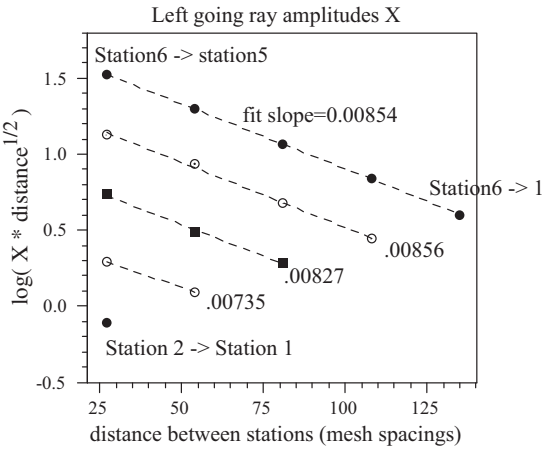

Fig. 4. Amplitudes of the left-going rays in the simulations – after correction for geometrical attenuation – versus interstation distance in units of mesh spacing. The upper five points (filled circles) correspond to the amplitudes from station 6 towards all the others. The next set of four symbols (circles with central dots) corresponds to the amplitudes from station 5 to stations 4, 3, 2, and 1. Filled squares correspond to the amplitudes from station 3 to stations 3, 2 and 1, and so forth. Dashed lines are linear fits (slope in units of nepers/mesh spacing). The known value is 0.0078.

Fig. 4. Amplitudes des rayons de la Fig. 3, allant vers la gauche (après correction de l'atténuation géométrique) en fonction de la distance interstations. Les lignes en pointillés sont des ajustements linéaires. La valeur connue est 0,0078.

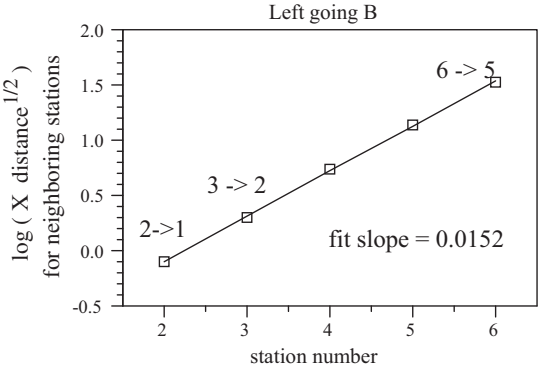

Fig. 5. The left-most data points of Fig. 4, i.e. the offsets between the lines, corresponding to the left-going intensities B at stations 2 through 6, are seen to diminish with distance across the array like exp(−2α * distance along array), as predicted by the radiative transfer equation. The solid line is a best fit.

Fig. 5. Les points les plus à gauche de la Fig. 4 correspondant à des intensités B qui vont à gauche dans les stations de 2 à 6, diminuent avec la distance au travers du réseau comme exp (−2α distance), tel que le prédit l'équation de transfert radiatif. La ligne continue est le meilleur ajustement.

both more restrictive than necessary and less restrictive than they could be. They are overly restrictive in that a straight line is appropriate only for identical site factors s and attenuation that is constant across the array. They are insufficiently restrictive in that separate fits for different originating stations (the four straight lines of Fig. 4), and for right-going and left-going waves, do not constrain the attenuation to be only a function of position $\vec{r}$. To illustrate a more general retrieval, the full set of all 30 amplitudes X was inverted by singular value decomposition for the B at the ends of the arrays, the site factors, and the interstation attenuations, twelve parameters in all. (The S were assumed to be zero).

Equation (3) was put in a form that represents the (log of the) $B^{\pm}$ at each of the stations as linear functions of the five interstation attenuations $\left(\int_{x_i}^{x_{i+1}} \alpha dx\right)$ and the (log of) B^{+} at the left end and the (log of) B^{-} at the right end. Similarly Eq. (1) was put in a form representing the (logs of the) $X_{ij}\,|x_i - x_j|^{1/2}$ as linear functions of the log s, the log B, and the five interstation attenuations. Combining these, one represents the (thirty distinct) $\log X_{ij}\,|x_i - x_j|^{1/2}$ as linear functions of the (six) log s, the (five) interstation attenuations and the (two) end intensities $B^{\pm}$. The sum of the log s was set to zero by absorbing an unknown scaling into the B. The resulting set of 30 linear equations in twelve parameters was pseudo-inverted by singular value decomposition, essentially a linear least squares procedure with uniform weighting.

This inversion procedure does not assume equal site factors s or uniform attenuation, nevertheless each site factor was correctly retrieved to within 2% of its known value (unity), and each interstation attenuation was correctly retrieved to within 10% of its known value $\left(0.211 = \int_{x_i}^{x_{i+1}} \alpha dx = 0.0078 \times 27\right)$. The inversion demonstrates recovery of independent site factors and independent interstation attenuations from correlations amongst a linear array of stations (for the case in which there are no sources S internal to the array). It thus endorses Eqs. (1–3) and correspondingly endorses the theoretical basis for retrieval of site factors and attenuations and specific intensities B in more general circumstances.

5. The effect of one-bit preprocessing

To reduce the influence of earthquake signals and to enhance the strength and bandwidth of the ambient noise correlations, ambient noise correlation studies have commonly applied data preprocessing that includes temporal normalization and spectral whitening. Lacking this, days of high noise intensity can dominate the averages and reduce the effective record length far below the nominal months. Lacking this, a record of months may be dominated by a few earthquakes and represent more the correlations of signals from a few point sources than a diffuse field. Common methods of temporal normalization include one-bit (Larose et al., 2004) and normalization using a running average. See Benson et al. (2007) for tests on preprocessing techniques. These data processing methods have been demonstrated to be highly effective at accelerating the convergence of the correlations and improving their signal-to-noise ratios.

However, such severe nonlinear preprocessing can cause problems in amplitude retrieval. Studies have shown that true amplitude may be poorly recovered after one-bit preprocessing when the ambient noise is not uniform (Cupillard and Capdeville, 2010; Larose et al., 2007). It has been suggested that amplitude information would be best recovered using raw data. The cost on the signal-to-noise ratio of doing this can be severe, however, and there may be other approaches.

The effects of one-bit operations on the amplitude of the correlation are difficult to quantify precisely. Nevertheless, it is clear why one-bit preprocessing distorts the ray amplitudes. Following the procedures of Cupillard et al. (2011) using their concepts of incoherent and coherent intensity and assuming the latter dominates, it is possible to show that the apparent amplitude of a ray arrival from site i to j after doing one-bit preprocessing is proportional to

$$X_{i\to j} \propto B_i(\hat{\mathbf{n}}_{i\to j})\,\frac{\exp(-|\int \alpha dx|)}{|\vec{r}_i - \vec{r}_j|^{1/2}} \Big/ \sqrt{\oint B_i(\hat{\mathbf{n}})d\hat{\mathbf{n}} \oint B_j(\hat{\mathbf{n}})d\hat{\mathbf{n}}} \tag{8}$$

(This follows from Cupillard et al. (2011)'s equation 52 after recognizing that the arguments of their arctangents are large when incoherent noise dominates, and on recognizing that the coherent and incoherent noise variances may be identified with the on-strike B and $\oint B_j(\hat{\mathbf{n}})d\hat{\mathbf{n}}$ respectively). The one-bit preprocessing has removed the site factors and normalized the correlation by the geometric mean of the total noise at the two stations. Equation (8) shows that the amplitude at receiver station j is affected by the usual geometric and exponential attenuations, but also through a factor of the inverse square root of the total noise power at j, $\left[\left(\oint B_j(\hat{\mathbf{n}})d\hat{\mathbf{n}}\right)\right]^{-1/2}$. If this factor is spatially constant, the relative values of the X are unaffected and attenuation ought be retrievable; such was reported by Cupillard and Capdeville (2010). If

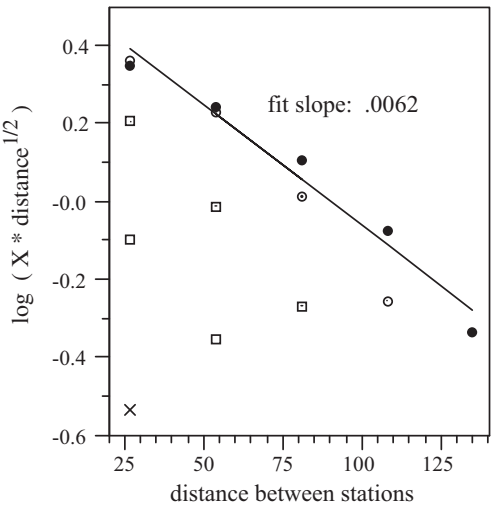

Fig. 6. Amplitude decay in the correlations obtained after one-bit preprocessing of the simulated data. This figure should be compared with Fig. 4 from band-passed raw data without one-bit preprocessing. Symbols are defined as in Fig. 4.

Fig. 6. Atténuation d'amplitude dans les corrélations obtenues après prétraitement *one-bit* des données simulées. On doit comparer cette figure avec la Fig. 4, à partir de données brutes de la bande de transmission sans prétraitement *one-bit*. Les symboles sont les mêmes que sur la Fig. 4.

incoherent noise is highly inhomogeneous, this factor can vary substantially with j, and the influence of attenuation $\exp(-|\int \alpha dx|)$ on X will be obscured. If, for example, propagation away from a dominant source of the noise is analyzed, i.e, away from the coast in a long-period seismic application, the total noise at j, $\oint B_j(\hat{\boldsymbol{n}})d\hat{\boldsymbol{n}}$, will decay with distance from the coast approximately like exp(–$2\alpha \times$ distance). The denominator in Eq. (8) will therefore diminish approximately like exp(–$\alpha \times$ distance), and the apparent attenuation will be close to zero. If propagation towards the coast is analyzed, attenuation will seem to be up to twice what it ought to be. One-bit preprocessing will distort the apparent attenuation.

This is confirmed by applying one-bit preprocessing to the above simulated data, and seeing that attenuation is not correctly recovered (Fig. 6). The fitted slope, 0.0062, is smaller than the known value 0.0078. This is consistent with the above argument that apparent attenuation is smaller when analyzing propagation away from the chief source of the noise (intensity is stronger on the right side of Fig. 1). Fig. 6 also shows that the quality of the straight line fits is poor and that the prefactors $B(\hat{\boldsymbol{n}})$ do not diminish with distance along the direction $\hat{\boldsymbol{n}}$ like exp(–$2\alpha \times$ distance) as required by the RTE.

One-bit preprocessing is attractive because it mitigates the effects of transients and accelerates convergence when noise intensity varies in time. It is simple but it is not always necessary. In order to retain rapid convergence amidst time-varying noise intensity, while preserving the relative gains at different stations, a different procedure is suggested here. If noise intensity varies slowly, more slowly than the propagation time across the array, it should suffice to do narrow-band temporal "flattening", in which every station's band-limited signal is normalized by a running average of the array's *total* band-limited energy. Thus each station is treated equally so that relative amplitudes are preserved. Furthermore, one day of high noise will not dominate a month's averaging. In practice this recipe may call for rejection of periods of high amplitude transient seismic activity.

To demonstrate the procedure, new numerical simulations were conducted using the same parameters as above but with noise intensity increased by a factor of 16 for $1/16^{\text{th}}$ of the time. Correlations were then generated using both the raw data and the flattened data. The relative amplitudes X of the arrivals were essentially the same for these two cases (and the same as originally) showing that apparent attenuation is not affected by flattening. In fact, the correlations from the flattening were identical to those of the original case using temporally-constant noise. The signal-to-noise ratio SNR, after preprocessing by flattening was also the same as originally. However, the SNR in the correlations of the raw data was degraded. Temporal flattening equalized the variable noise source, leading to faster convergence with all information being used, while (unlike one-bit preprocessing as in Fig. 6) preserving relative signal amplitudes between stations.

6. Summary

Disentangling the many factors affecting correlation amplitudes in order to reliably recover attenuation is challenging. It has been argued here that one key factor, noise intensity, or ponderosity, may be modeled by a radiative transfer equation and that this recognition is sufficiently constraining that we may hope to fit measured correlation amplitudes and retrieve attenuation, at least for the linear detector arrays considered here. Further work will require extending these ideas to two-dimensional arrays, to the case in which noise intensity is augmented by sources P and scattering p, to incorporating knowledge of confidence levels on the correlation amplitudes (essentially the SNR) so as to properly weight least squares minimization, and to the effects of focusing and defocusing due to spatially varying wavespeed.

Acknowledgements

The author's work was supported by a contract from Los Alamos National Laboratory. He thanks Xiaodong Song for helpful discussions, and in particular for performing the singular value decomposition pseudo inverse.

References

Aki, K., 1957. Space and time spectra of stationary stochastic waves, with special reference to microtremors. Bull. Earthq. Res. Inst. 35, 415–457.

Benson, G., Ritzwoller, M., Barmin, M., Levshin, A.L., Lin, F., Moschetti, M.P., Shapiro, N.M., Yang, Y., 2007. Processing seismic ambient noise data to obtain reliable broad-band surface wave dispersion measurements. Geophys. J. Int. 169, 1239–1260.

Cupillard, P., Capdeville, Y., 2010. On the amplitude of surface waves obtained by noise correlation and the capability to recover the attenuation: a numerical approach. Geophys. J. Int. 181, 1687–1700.

Cupillard, P., Stehly, L., Romanowicz, B., 2011. The one-bit correlation: a theory based on the concepts of coherent and incoherent noise. Geophys. J. Int. 184, 1397–1414.

Derode, A., Larose, E., Tanter, M., de Rosny, J., Tourin, A., Campillo, M., Fink, M., 2003. Recovering the Green function from field-field correlations in an open scattering medium. J. Acoust. Soc. Am. 113, 2973–2976.

Froment, B., Campillo, M., Gouedard, P., Roux, P., Weaver, R.L., Verdel, A., 2010. Estimation of the effect of non-isotropically distributed energy on the apparent arrival time in correlations. Geophysics 75, SA85.

Godin, O., 2009. Accuracy of the deterministic travel time retrieval from cross correlation of non diffuse ambient noise. J. Acoust. Soc. Am. 126, EL183–EL189.

Larose, E., Derode, A., Campillo, M., Fink, M., 2004. Imaging from one-bit correlations of wide-band diffuse wavefields. J. Appl. Phys. 95, 8393–8399.

Larose, E., Roux, P., Campillo, M., 2007. Reconstruction of Rayleigh-Lamb dispersion spectrum based on noise obtained from an air-jet forcing. J. Acoust. Soc. Am. 122, 3437–3444.

Lin, F.C., Moschetti, M.P., Ritzwoller, M.H., 2008. Surface wave tomography of the western United States from ambient seismic noise: Rayleigh and Love wave phase velocity maps. Geophys. J. Int. 173, 281–298.

Lobkis, O.I., Weaver, R.L., 2001. On the emergence of the Green function in the correlations of a diffuse field. J. Acoust. Soc. Am. 110, 3011–3017.

Malcolm, A.E., Scales, J.A., van Tiggelen, B.A., 2004. Extracting the Green function from diffuse, equipartitioned waves. Phys. Rev. E 70, 015601.

Prieto, G.A., Beroza, G.C., 2008. Earthquake ground motion prediction using the ambient seismic field. Geophys. Res. Lett. 35, L14304.

Prieto, G.A., Lawrence, J.F., Beroza, G.C., 2009. Anelastic Earth structure from the coherency of the ambient seismic field. J. Geophys. Res. 114, B07303.

Roux, P., Sabra, K.G., Kuperman, W.A., Roux, A., 2005a. Ambient noise cross correlation in free space: Theoretical approach. J. Acoust. Soc. Am. 117, 79–84.

Roux, P., Sabra, K.G., Gerstoft, P., Kuperman, W.A., Fehler, M.C., 2005b. P-waves from cross-correlation of seismic noise. Geophys. Res. Lett. 32, L19303.

Ryzhik, L., Papanicolaou, G., Keller, J.B., 1996. Transport equations for elastic and other waves in random media. Wave Motion 24, 327–370.

Sabra, K.G., Gerstoft, P., Roux, P., Kuperman, W.A., Fehler, M.C., 2005. Surface wave tomography from microseisms in Southern California. Geophys. Res. Lett. 32, L14311.

Shapiro, N.M., Campillo, M., Stehly, L., Ritzwoller, M.H., 2005. High-resolution surface-wave tomography from ambient seismic noise. Science 307, 1615–1618.

Snieder, R., 2004. Extracting the Green function from the correlation of coda waves: q derivation based on stationary phase. Phys. Rev. E 69, 046610.

Turner, J.A., Weaver, R.L., 1994. Radiative transfer of ultrasound. J. Acoust. Soc. Am. 96, 3654–3674.

Wapenaar, K., 2004. Retrieving the elastodynamic green's function of an arbitrary inhomogeneous medium by cross correlation. Phys. Rev. Lett. 93, 254301.

Weaver, R.L., 2005. Perspectives geophysics "Information from Seismic Noise". Science 307, 1568.

Weaver, R.L., 2011. Towards Green function retrieval from imperfectly partitioned 2-d ambient wave fields: travel times, attenuations, specific intensities, and scattering strengths. In: Hutter, K., Tsung-Tsong Wu, Yi-Chung Shu (Eds.), From Waves in Complex Systems to Dynamics of Generalized Continua – Tributes to Professor Yih-Hsing Pao on his 80th Birthday, World Scientific.

Weaver, R.L., Lobkis, O.I., 2001. Ultrasonics without a source. Thermal fluctuation correlations at MHz frequencies. Phys. Rev. Lett. 87, 134301.

Weaver, R.L., Lobkis, O.I., 2004. Diffuse waves in open systems and the emergence of the Greens' function. J. Acoust. Soc. Am. 116, 2731–2734.

Weaver, R.L., Froment, B., Campillo, M., 2009. On the correlation of non-isotropically distributed ballistic scalar diffuse waves. J. Acoust. Soc. Am. 126, 1817–1826.